Living on the edge – physiological tolerance to frost and drought explains range limits of 35 European tree species

Anne Baranger, Thomas Cordonnier, Guillaume Charrier, Sylvain Delzon, Maximilian Larter, Nicolas K Martin-Stpaul, Georges Kunstler

ECOGRAPHY

Research article

Living on the edge – physiological tolerance to frost and drought explains range limits of 35 European tree species

Anne Baranger[1], **Thomas Cordonnier**[1,2], **Guillaume Charrier**[3], **Sylvain Delzon**[4], **Maximilian Larter**[4], **Nicolas K. Martin-StPaul**[5] **and Georges Kunstler**[1]

[1]INRAE, LESSEM, Univ. Grenoble Alpes, St. Martin-d'Heres, France
[2]Office National des Forêts, Recherche Développement et Innovation, Dole, France
[3]INRAE, PIAF, Univ. Clermont Auvergne, Clermont–Ferrand, France
[4]INRAE, BIOGECO, Univ. de Bordeaux, Pessac, France
[5]INRAE, URFM, Avignon, France

Correspondence: Anne Baranger (annebarang@gmail.com)

Ecography
2024: e07528
doi: 10.1111/ecog.07528

Subject Editor: Carissa Brown
Editor-in-Chief: Miguel Araújo
Accepted 31 October 2024

Species distribution models are key to evaluate how climate change threatens European forests and tree species distributions. However, current models struggle to integrate ecophysiological processes. Mechanistic models are complex and have high parameter requirements. Some correlative species distribution models have tried to include traits but so far have struggled to directly connect to ecophysiological processes. Here, we propose a new strategy in which species distributions are based on safety margins which represent species' proximity to their physiological thresholds. We derived frost and drought safety margins for 38 European tree species as the difference between physiological tolerance traits and local maximum stress. We used LT_{50} and Ψ_{50} as tolerance traits for frost and drought, respectively, and local minimum temperature and minimum soil water potential as maximum stress. We integrated these safety margins into a species distribution model, which tests if the probability of species presence declines rapidly when the safety margin reaches zero, when physiological stress exceeds the species' tolerance traits. Our results showed thaet 35 of the 38 studied species had their distribution explained by one or both safety margins. We demonstrated that safety-margins-based model can be efficiently transferred to species for which occurrence data are not available. The probability of presence dropped dramatically when the frost safety margin reached zero, whereas it was less sensitive to the drought safety margin. This differential sensitivity may be due to the more complex regulation of drought stress, especially as water is a shared resource, whereas frost is not. Our analysis provides a new approach to link species distributions to their physiological limits and shows that, in Europe, frost and drought safety margins are important determinants of species distributions.

Keywords: LT50, minimum soil water potential, minimum temperature, P50, physiological limits, safety margins, species distribution, tolerance traits

NORDIC SOCIETY OIKOS

www.ecography.org

Introduction

Climate change is a major threat to European forests and has already led to significant changes in species ranges, forest structure and consequently ecosystem services (Lindner et al. 2014). A common way to assess this vulnerability is through correlative species distribution models (SDMs), which correlate species occurrence data with climate drivers to estimate shifts in species distributions (Elith and Leathwick 2009). However, the advent of new climatic conditions, particularly at the hot edge of species distributions, leads to extrapolation of SDM outside their calibration range, often resulting in low predictive performance (Nguyen and Leung 2022). To overcome extrapolation issues, mechanistic models attempt to explicitly represent key physiological processes that control species persistence (Chuine and Beaubien 2001, Venturas et al. 2021, Ruffault et al. 2022). Despite increasing transferability in time and space, mechanistic models require extensive parameter estimation for each species, which limits their application to a few species (Dormann et al. 2012). This is why recent research has sought to integrate plant functional traits into correlative SDMs in order to include external information on species ecological strategies and connect SDMs with mechanistic models (Pollock et al. 2012, Vesk et al. 2021). In this approach (referred hereafter as traits-SDM) functional traits modulate species' response to the environment, which facilitates the transfer of models to species for which only the traits are known (Vesk et al. 2021). Yet the processes determining the trait–environment relationship are usually not explicit and are inferred only in post hoc analyses. This is mostly because the traits that are commonly measured and classically used in traits-SDM, such as specific leaf area, maximum height or wood density (Pollock et al. 2012), are integrative traits that have complex drivers and are not directly linked to environmental constraints. Because of this, connecting traits-SDM models with the mechanistic ecophysiological processes controlling species distribution remains difficult.

In recent years, there has been an increased availability in physiological tolerance traits that directly quantify the tolerance thresholds of plants. These new traits offer a path to a tighter connection with ecophysiological processes, but this requires moving SDMs from classical climate space to the space of the physiological stress experienced by the species (Choat et al. 2018, Dormann et al. 2012). To do this, one way is to convert the environmental drivers into physiological stresses: the distance between the local maximum physiological stress and the physiological tolerance trait of the species defines a safety margin, i.e. a quantification of the local risk of crossing an ecophysiological limit (Martínez-Vilalta et al. 2021). Fitting correlative SDMs in this safety margins space would enable to link directly traits to physiological processes without modelling the full complexity of ecophysiological processes. More specifically, this would allow us to test if species' probability of presence decreases as they approach their physiological limits in safety margin space. In this approach, model parameters would be directly linked to traits, in particular, quantify whether excessive stress (i.e. negative safety margin) induces a drop in probability of presence. Such a safety margin-based model would provide a foundation for a generic species distribution model, which would enable to predict species's distributions solely based on their traits.

In Europe, frost and drought are primary physiological stresses shaping tree species distributions (Lindner et al. 2014). These stresses act through multiple physiological processes (Anderegg et al. 2015, Körner et al. 2016), thus species' tolerance to frost and drought can be tricky to capture.

Concerning frost, it can reduce fitness because freeze–thaw cycles lead to hydraulic failure or because low temperatures provoke extracellular ice causing cell lysis and tissue death both in spring and in winter (Sakai and Larcher 1987, Körner et al. 2016). There are currently no standardised traits for comparing resistance to freeze–thaw-induced embolism across a large number of species (Charrier et al. 2017). Cell tolerance to cold-induced lysis can be measured as the temperature at which 50% of cells are lysed, so-called LT_{50}. It is a dynamic trait that decreases during cold acclimation, reaches a minimum value in deep winter and then rises during cold deacclimation in spring (Sakai and Larcher 1987, Charrier et al. 2013, 2017). This temporal dynamics makes it more difficult to measure LT_{50} in a standardised way during spring for a large number of species, as it largely depends on local temperature dynamics, whereas standardisation is easier for winter LT_{50}. We propose here to focus on winter maximum frost hardiness, considering this trait as static in contrast with tolerance to spring frost events and freeze–thaw induced embolism.

Concerning drought, it can cause stomata closure and limit growth (Martin-StPaul et al. 2017), or inflict excessive tension on the plant's water column, causing embolism of the conduits and leading to hydraulic failure. The latter is often recognised as a major cause of forest mortality during severe drought (Anderegg et al. 2015, but see Mantova et al. 2022 for a debate about the exact mechanisms at play). Ψ_{50} is a trait that assesses plants' resistance to hydraulic failure by measuring the water potential that causes a 50% loss in hydraulic conductivity due to drought-induced embolism. We now have large databases on Ψ_{50} allowing the classification of species resistance to droughtinduced hydraulic failure (Choat et al. 2012, Martin-StPaul et al. 2017, Hammond et al. 2021).

To our knowledge, no studies have explored direct links between LT_{50} and Ψ_{50} and species distribution. Yet, several studies have shown correlations of LT_{50} and Ψ_{50} with stress-induced mortality (Charra-Vaskou et al. 2012, Anderegg et al. 2015, Trugman et al. 2021), although this has been done only for a few species for LT_{50} (Scots pine, Lindström et al. 2014, Douglas-fir, Timmis et al. 1994). Some studies have also reported correlations between Ψ_{50} or LT_{50} and species mean climate or rough indicators of species climatic range limits (Charrier et al. 2013, Larter et al. 2017, Sanchez-Martinez et al. 2020, Skelton et al. 2021). Most of these studies were not based on explicit estimation of safety margin but just on classical climatic variables. More recently,

some studies have modelled the risk of drought hydraulic damage at the tree level in the US (Venturas et al. 2021, with a mechanistic model) or in France and Spain (Benito Garzón et al. 2018, with drought safety margins) and found it to explain, respectively, 2% and 27% of the variance in mortality. Sanchez-Martinez et al. (2023) assessed drought hydraulic risk at the community level (based on phylogenetically imputed species average safety margins) and found a significant relationship with drought-induced mortality. Some studies have explored the relationship between the spring frost safety margin and species' upper elevation limits for a few tree species in the Alps (Lenz et al. 2013). But to our knowledge, no studies have used both frost and drought tolerance traits to build SDMs in a multidimensional safety margin space at the continental scale.

Here we propose to build on recent advances in the measurement of Ψ_{50} and LT_{50}, together with the availability of large-scale climate data (Muñoz-Sabater et al. 2021), to derive continent-wide frost and drought safety margins across Europe for 38 European tree species. When included in a SDM, this allows us to test whether there is a sudden drop in the probability of presence when a species crosses its threshold of zero safety margin, i.e. when the physiological stress exceeds its tolerance (Fig. 1), and therefore whether Ψ_{50} and LT_{50} are relevant to delineate species distributions. More specifically, our analysis tests the following hypotheses: 1) species' maximum experienced frost or drought stress better explains the interspecific variation in LT_{50} and Ψ_{50} than classical climatic variables; 2) parameters of the fitted SDM indicate a drastic and non-linear drop in the probability of species presence as the safety margins decrease, and the drop occurs at the zero safety margins of the species; 3) models based on safety margins can be transferred to species with only traits and no occurrence to predict their distribution.

Material and methods

We compiled published data on drought and frost physiological tolerance traits for the main European tree species and complemented missing species with new measurements. Using climate reanalysis and soil hydraulic parameter maps, we computed proxies of longterm maximum frost or drought stress for all cells of a European tree species occurrence database. These allowed us to estimate both species' maximum experienced drought and frost stress throughout their distribution and how species-specific safety margins vary within the species distribution. These safety margins were used to build bivariate logistic species distribution models (Fig. 1).

Study area and species presence data

The study was carried out on 38 tree species naturally occurring in Europe (Supporting information) for which physiological traits and more than 400 occurrence points were available. These species are distributed in forest biomes ranging from the Mediterranean to the boreal forest.

Physiological tolerance thresholds for frost and drought

Species-specific stress tolerance traits are estimated as the level of stress at which irreversible damage is reached (generally 50% of damage). They are extracted from sigmoid vulnerability curves fitted to experimental data of damage measurements at different stress levels. For each species, we took the average of all measurements from our compilation of published data and additional measurements (details per traits below).

Frost tolerance

We collected estimates of LT_{50} (the temperature causing 50% of cell lysis) from various published and unpublished data (Supporting information). As we focused on winter frost tolerance to control for seasonal variation in frost tolerance (LT_{50}), we used measurements taken in winter, when all species exhibit maximum frost tolerance. We selected only measurements that were performed using either the electrolyte leakage or visual scoring method, on adult trees, and on branches or buds. For 23 species for which LT_{50} data were

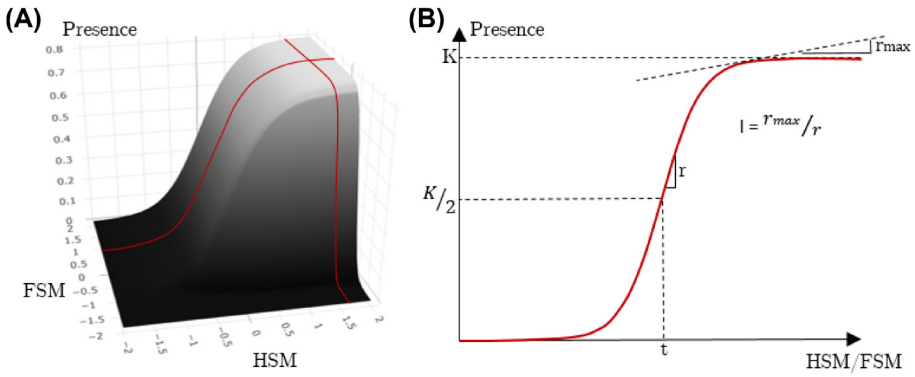

Figure 1. Logistic model for the probability of species presence. (A) The probability of presence is represented as a bivariate function of FSM and HSM. If one of the two safety margins is limiting, the probability of presence drops. (B) The red transects in (A) are plotted in one dimension with key parameters of the model. The inflection index *I* and its calculation are also shown.

not available in the literature or of low quality, additional measurements were made to complete the database (see the Supporting information for details).

Drought tolerance

We extracted from global databases estimates of the xylem pressure (i.e. water potential) at which the percentage of embolized conduits exceeds the critical threshold of hydraulic failure (Choat et al. 2012, Martin-StPaul et al. 2017, Hammond et al. 2021, Supporting information) (Ψ_{crit}). We filtered out Ψ_{crit} measurements with non-sigmoid vulnerability curves. We chose measurements from adult tree stems to avoid the ontogenic effects observed with saplings grown in pots. Previous studies have suggested that the threshold of embolism leading to hydraulic failure differs between gymnosperms and angiosperms (Urli et al. 2013). Based on this, we used a critical threshold of 50% for gymnosperms (Ψ_{50}) and 88% for angiosperms (Ψ_{88}) as the point of no return.

Estimation of long-term maximum stresses and safety margins

The frost and drought hydraulic safety margin (FSM, HSM) are the difference between the physiological tolerance threshold and the long-term maximum experienced stress at a given location.

There are several approaches to estimating frost and drought maximum stress. For frost, the maximum stress is related to the extreme minimum temperature (even during a short period and with a long return interval). Thus, we used long-term hourly temperature reanalysis time series to extract extreme low-temperature events. We acknowledge that the temperature experienced by a tree can deviate from air temperature by several degrees, but no data allows us to go into such detail for the moment. For drought, the minimum tree water potential at midday – measured in the field – is most commonly used as a proxy for maximum stress and compared to Ψ_{crit} (Choat et al. 2012, Sanchez-Martinez et al. 2023). However, this approach cannot be used at the scale of a species' distribution because minimum water potentials are only available for a few locations. Instead, we determined the maximum drought stress based on the minimum soil water potential (Ψ_{min}) from long-term reanalysis of soil water content (θ). Assuming that tree and soil water potentials are in equilibrium when stomata are closed to control water loss, Ψ_{min} is a proxy for the maximum experienced stress (Martínez-Vilalta et al. 2021).

Long-term climatic minimum

We used hourly time series of temperature and soil water content (θ) between 1984 and 2021 taken from the ERA5 Land dataset at 9 × 9 km resolution (Muñoz-Sabater et al. 2021). For each variable, location and year, we computed the annual maximum stress as the minimum of the annual time series. Then to estimate the long-term maximum stress of frost and drought (T_{min} and θ_{min}) while limiting the effect of outliers, we computed the 5th percentile of the time series of annual minimum temperature and θ. The 5th percentile is equivalent to a 20-years return rate.

Derivation of minimum soil water potential from soil water content

Ψ_{min} depends on the minimum soil water content (θ_{min}), soil hydraulic properties (mainly driven by texture) at each location, and root distribution. For each of the four soil horizons (ranging from 0 to 2.8 m) and cell of the ERA5 Land dataset (Muñoz-Sabater et al. 2021) we computed θ_{min} with the method presented above. Then, we used the Van Genuchten pedotransfer functions to calculate Ψ_{min} for each horizon h (Van Genuchten 1980, Supporting information) using the following equation:

$$\bar{\theta}_{\min,h} = \frac{\theta_{\min,h} - \theta_r}{\theta_s - \theta_r} \quad (1)$$

$$\Psi_{\min,h} = \left[\left(\frac{1}{\theta_{\min,h}}\right)^{1/m} - 1\right]^{1/n} \times \frac{1}{\alpha} \quad (2)$$

Where $\theta_{min,h}$ is the minimum soil water content, $\bar{\theta}_{min,h}$ is the reduced water content, θ_r, θ_s, α, n and m are hydraulic parameters. We extracted hydraulic parameters from Tóth et al. (2017) 1 × 1 km soil hydraulic parameter maps, which provide parameters for seven horizons from 0 to 2.8 metres deep based on soil information data. We matched each of the latter seven horizons to one of the four horizons from ERA5 land (Supporting information).

We used the root module of the SurEau-ECOS model (Ruffault et al. 2022) to weight the contribution of the water potential of each horizon based on their hydraulic conductivity and fine roots density distribution to compute a value close to the soil water potential experienced by the tree root system. First, using the Van Genuchten hydraulic conductivity curve, we calculated the unsaturated hydraulic conductivity of each horizon h, where :

$$K_{\min,h} = K_0 \cdot \left(\bar{\theta}_{\min,h}\right)^L \cdot \left(1 - \left(1 - \bar{\theta}_{\min,h}^{1/m}\right)\right)^m \quad (3)$$

With K_0, m and L hydraulic parameters extracted from (Tóth et al. 2017). Then, K_{min} was scaled to the width of the layer using the Gardener-Cowan coefficient, B_{GC} (Supporting information). B_{GC} modulates the conductance of the soil layer according to the density of fine roots in the layer; it depends on the root radius, the root distribution profile (depending on a root distribution index β, details in the Supporting information), the root-to-leaf ratio, the leaf area index (LAI) and the maximum root depth at each location. Root radius, root-to-leaf ratio and LAI were set to 0.004 m, 1 and 5 m^2 m^{-2} respectively, according to the parameterization of SUREAU-ECOS (Ruffault et al. 2022). The maximum root depth at 1 × 1 km was extracted from Hiederer (2013).

Detailed calculation and sensitivity analysis of Ψ_{min} to B_{GC} parameters (LAI and β) are presented in the Supporting information. For each horizon h the rescaled potential was :

$$\Psi_{root,h} = \Psi_{min,h} \; K_{min,h} \; B_{GC,h} \quad (4)$$

Finally, $\Psi_{root,h}$ was computed for each horizon and then scaled to the total conductivity. The weighted Ψ_{min} experienced by the roots over the entire soil profile was:

$$\Psi_{min} = \frac{\sum_{h=1}^{7} \left[\Psi_{min,h} \cdot K_{min,h} \cdot BCG_h\right]}{\sum_{h=1}^{7} \left[K_{min,h}\right]} \quad (5)$$

Species distribution analysis

Presence/absence and climate data

We extracted presence/absence data from the EuForest database (Mauri et al. 2017), which is a 1 × 1 km grid, based on aggregated datasets. For each EuForest occurrence point, in addition to T_{min} and Ψ_{min}, we extracted from the CHELSA data (Karger et al. 2017) the annual sum of precipitation *map*, annual potential evapotranspiration *pet* and mean annual temperature *mat*. In order to ensure that differences in the resolution of the climatic data did not bias our comparison of the effect of climate niche extreme on tolerance traits, we aggregated CHELSA at the resolution of ERA5-land.

For each species, we determined whether the presence/absence EuForest dataset captured its distribution limit at the dry or cold margin. For instance, EuForest captures the dry margin of a species if it includes absence observations in dryer locations than the margin of the species. If this is not the case, it is not possible to tell whether the dry margin in EuForest data is an environmental margin or the limit of the dataset. We tested the coverage of each margin by comparing the 95th percentile of *pet* and the 5th percentile of *mat* between the presence and absence of each species (Supporting information). We tested the drop in the probability of presence only for the margins covered by the EuForest data.

Interspecific variation in species climatic niche extremes and their physiological tolerance traits

For each of the five climatic variables (*map*, *mat*, *pet*, T_{min} and Ψ_{min}) and each species, we computed its respective extreme (hereafter called climatic niche extremes) as the 5th percentile for *map*, *mat*, T_{min} and Ψ_{min} or the 95th percentile for *pet* over its distribution.

To test our first hypothesis that maximum experienced frost and drought stress explain interspecific variation in LT_{50} and Ψ_{50} better than classical climatic variables, we performed univariate linear regression of LT_{50} with climatic niche extremes of *mat* or T_{min} and of Ψ_{crit} with the climatic niche extremes of *map*, *pet* or Ψ_{min}. We used t-tests to test whether the regression coefficients were significantly non-null. R^2 of the regression and effect-size (computed as standardised coefficients, Schielzeth 2010) were used to quantify the strength of the relation between climatic niche extremes and species physiological tolerance traits.

Distribution models and safety margins

Species-specific distribution models

Species j presence/absence in each 1 × 1 km grid cell i was modelled assuming a Bernoulli distribution with a probability of presence $p_{i,j}$.

We modelled $p_{i,j}$ as being limited by both safety margins with logistic functions to allow for a drastic drop in probability of presence at low safety margins. The shape of the model itself tests the relevance of the zero safety margin threshold. To represent that a high probability of presence occurs only in areas where neither frost nor drought is limiting, we formulated the model as a multiplicative function of the two logistic functions as:

$$p_{i,j} = \frac{K_j}{\left[1+\exp\left(-r_{FSM,j}\cdot\left(FSM[i,j]-t_{FSM,j}\right)\right)\right]\cdot \left[1+\exp\left(-r_{HSM,j}\cdot\left(HSM[i,j]-t_{HSM,j}\right)\right)\right]} \quad (6)$$

with $t_{FSM,j}$, $r_{FSM,j}$ and K_j being model estimated parameters, j the species and i a grid cell. The t parameters correspond to an offset on the safety margins and its value is key to testing the relevance of physiological tolerance trait. If negative, the species can tolerate physiological stress and is present even with negative safety margins (Fig. 1). If positive, the species probability of presence starts to decrease even when safety margins are positive. The t parameters were constrained to the observed interval of the corresponding safety margins, and we assumed a normal prior centred around 0 with a standard deviation of 1. The r parameters correspond to the slope at the inflection point at the threshold t. The larger r, the more sensitive the species is to its margin of safety. The r parameters were restricted to positive values to force safety margins to have a positive link with higher presence rates or no effect. K_j is the maximum probability of presence when both safety margins are favourable to the species. The K_j parameters are inherently between 0 and 1, and a normal distribution prior was set. We used an informative prior for the mean based on the mean probability of presence of the species in its EuForgen distribution and a standard deviation of 1.

We also explored alternative simpler models where the probability of presence p_i is related only to HSM, or to FSM, or none (Supporting information).

For each species, we only fitted models that included the safety margins for which the EuForest data covered their respective climatic margins (FSM for cold margin and HSM for dry margin). In other words, for a species for which no absence data could cover the cold limit, we did not fit a model that included the FSM. Models were inferred using the Bayesian statistical paradigm with the 'Rstan' package (Carpenter et al. 2017). All other statistical analyses were performed using R software (www.r-project.org).

Model selection and index

We first discarded models with poor convergence based on two criteria: more than 1% of divergent transitions during sampling of the four chains and potential scale reduction factor – *RHat* > 1.1 (Gelman et al. 2013). Then, for each species, we selected the model with the lowest Bayesian information criterion – BIC (Schwarz 1978) among the converging models. The difference in BIC with the next best model was always greater than 2 indicating strong support for the selected model (Supporting information).

We computed AUC (Fielding and Bell 1997) for each model using the model predictions over the data used in the fit. AUC measures the fit quality, 0.5 being the AUC of a random model and 1 of a perfect fit.

We calculated an inflection index I to assess the strength of the drop of the species probability of presence along FSM or HSM, based on the ratio between the slope at the 95th percentile of the safety margin and the slope at the inflection point (r). The inflection index was one minus the ratio and ranged between 0 and 100%. The higher I, the more non-linear the model (Fig. 1). To facilitate the comparison of t_{hsm} and t_{fsm}, we derived rescaled thresholds. We scaled the t parameters to the range of safety margins covered by each species.

Transferability of generic safety margins-based to 'unobserved species'

Because safety-margin-based distribution models incorporate species-specific physiological tolerance traits, they should have a good ability to predict species for which no occurrence observations were used in the fit ('unobserved species'). To assess transferability, we repeatedly calibrated a generic model on all species except one and predicted the distribution of this 'unobserved' species with the corresponding model (in total we fitted 38 generic models). For the generic models we use the same structure as Eq. 6 but with a random species effect on the asymptote K_j (assuming a beta distribution), to account for differences between species, as:

$$p_{i,j} = \frac{K_j}{\left[1+\exp\left(-r_{\mathrm{FSM}}\cdot\left(\mathrm{FSM}[i,j]-t_{\mathrm{FSM}}\right)\right)\right]\cdot \left[1+\exp\left(-r_{\mathrm{HSM}}\cdot\left(\mathrm{HSM}[i,j]-t_{\mathrm{HSM}}\right)\right)\right]} \quad (7)$$

$$K_j \sim B\left(\lambda\cdot K, \lambda\cdot(1-K)\right) \quad (8)$$

with t_{FSM}, r_{FSM}, K_j, K and λ being model estimated parameters, j being the species and i the grid cell. K being the mean random asymptote of all species, λ a shape parameter, and r and t are common to all species (see the Supporting information for model details). We assessed the ability of a generic model to predict the distribution of an unobserved species using the true skill statistic (TSS) (Allouche et al. 2006) and the average AUC over all unobserved species (Fielding and Bell 1997). Higher TSS and AUC closer to 1 indicates a better prediction quality. We used only 31 generic models because the other 7 models led to convergence issues.

Results

Frost and drought tolerance traits are strongly correlated with maximum experienced stresses

We found that frost and drought tolerance traits (Ψ_{crit} and LT_{50}) were correlated with climatic niche extremes based on physiological stress, the effects being equal or slightly stronger than for climatic niche extremes based on classical climatic variables. For Ψ_{crit}, we observed that the minimum soil potential extreme (i.e. 5th percentile of Ψ_{min}) has the strongest effect (standardised regression coefficient and its 95% confidence interval: 0.77 [0.29, 1.24]; $p < 0.01$; Fig. 2). This suggests that trees have lower Ψ_{crit}, thus higher resistance to xylem embolism, when their niches extend into extremely low soil moisture. Potential evapotranspiration extremes *pet* also correlated with Ψ_{crit}, with higher *pet* correlated with more resistant species. Finally, we found that low precipitation extremes had no correlation with Ψ_{crit}. We also tested the effect of *map* − *pet*, which is a classical aridity index, but found no effect.

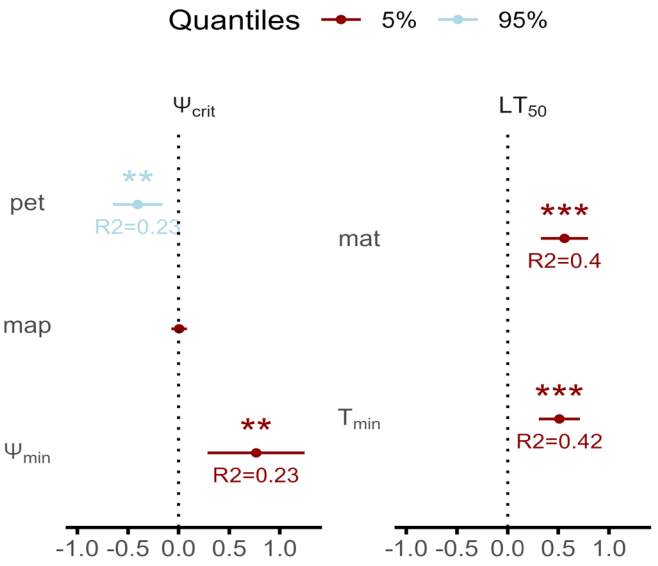

Figure 2. Standardised coefficients of the regression of physiological tolerance traits against climatic niche extremes. The climatic niche extreme is estimated using climatic variables (5th percentile of mean annual precipitation *map* and mean annual temperature *mat*, 95th percentile of annual potential evapotranspiration *pet*) or maximum experienced stress (5th percentile of minimum temperature T_{min} and minimum soil potential Ψ_{min}). Ψ_{crit} refers to Ψ_{50} (gymnosperms) or Ψ_{88} (angiosperms). The analysis includes all species for which the occurrence data cover the corresponding margin of the distribution. *, ** and *** indicate a significant relationship with p-values less than 0.05, 0.01 and 0.001, respectively. Bars indicate 95% confidence intervals.

For LT_{50}, we observed an equivalent effect of extreme low temperature (i.e. 5th percentile of T_{min}; 0.51 [0.31, 0.71]; Fig. 2) and extreme mean annual temperature (i.e. 5th percentile of *mat*; 0.56 [0.33, 0.80]; Fig. 2). This led to lower LT_{50} with decreasing T_{min} and *mat*. These effects were both significant and positive ($p < 0.001$ for both T_{min} and *mat*).

We also investigated correlations between all the climatic niche extremes and found correlations greater than 0.9 between Ψ_{min} and *pet*, and between T_{min} and *mat* (Supporting information)

Species probability of presence are related to their safety margins

Our results show that for species for which occurrence data covered their frost or drought margin, the corresponding safety margin was generally selected in models over the null model.

In particular, among the 30 species that had absence/presence distribution data that allowed us to test the effect of FSM, 26 had FSM selected in the final model. Similarly, among the 28 species that had absence/presence distribution data that allowed us to test the effect of HSM, all of them had HSM selected in the final model. Within these two groups of species, we tested both safety margins for 23 species and found that 19 of them were indeed explained by both FSM and HSM. Out of the 38 species, the distribution of only three species could not be explained by their safety margins (*Juniperus communis*, *Populus alba* and *Quercus pubescens*). The mean AUC of all models was 0.69, with 25 species having AUC over 0.65 indicating acceptable fits, and six of which had particularly good fits with AUC over 0.8. The ten other species had low AUC (< 0.65) which may be caused by their very low prevalence (median prevalence and quartiles of these 10 species: 0.017 [0.013, 0.04]; of the 25 other species: 0.11 [0.04, 0.22]).

Species probability of presence respond non-linearly to their safety margin

We observed that crossing the LT_{50} thresholds resulted in a drastic drop in the probability of presence, while the decrease was more progressive for Ψ_{50}. The rescaled thresholds of FSM (mean estimate of rescaled *t* with its 95% confidence interval: 0.04 [−0.01, 0.10]) were on average closer to zero than those of HSM (mean estimate of rescaled *t* with its 95% confidence interval 0.14 [0.01, 0.27], Fig. 3B). This means that the probability of species presence drops close to the point where the species frost tolerance LT_{50} is exceeded, while the thresholds for HSM are higher with wide confidence intervals. This large variability is mainly due to the angiosperm species. Moreover, the HSM thresholds of angiosperms are three times lower than those of gymnosperms, indicating a drop in the probability of presence closer to the point where the species' drought tolerance is crossed.

The inflection index *I* for FSM (Fig. 3B) was 10 times higher than for HSM, showing a stronger non-linearity compared to HSM (Fig. 3A).

Transferability of safety margin model for species without occurrence data

With a generic model based on safety margins, we found moderate predictive ability for a species not included in the model fit, *i.e.* 'unobserved species'. The mean AUC of predictions for each species was 0.67, with an inter-quartile range of 0.63–0.72. Only five species had an AUC below 0.6. This was close to AUC found for traits-SDM models (AUC median and inter-quartile of Vesk et al. (2021): 0.65 [0.57, 0.77]). The TSS also indicated good fit quality, with a mean TSS of 0.30 and an inter-quartile range of 0.23–0.40 (Supporting information). In addition, the sensitivity of the models was on average higher than their specificity (mean sensitivity and inter-quartile: 0.83 [0.79, 0.90], specificity: 0.47 [0.39, 0.58]), indicating a pattern of over-predicting presence over absence.

Discussion

Our attempt to combine frost and drought safety margins in correlative species distribution models showed that for 35 European tree species the probability of presence dropped when their tolerance thresholds were exceeded. In particular, the cold limit was close to a zero safety margin and corresponded to a strongly non-linear decrease in the probability of presence, whereas the probability of presence started to decrease more progressively at positive drought safety margins. Our model represents a new approach to including traits in SDMs, and demonstrates the relevance of physiological tolerance traits and safety margins to model species distribution. Interestingly, our correlative model based on safety margins performed well at predicting 'unobserved species', with prediction metrics being of the same order as previous traits-SDM.

Maximum experienced stresses explain inter-specific variability in physiological tolerance traits

Interspecific variations in frost and drought tolerance traits were explained by niche climatic extremes, and in particular by maximum experienced stress (Fig. 2). We found higher or equivalent effect-size between LT_{50} and Ψ_{50} and the extremes of their respective maximum experienced stress T_{min} and Ψ_{min} than with the more classical climatic variables *map*, *pet* and *mat*. Our results support our initial hypothesis that the maximum experienced stresses are closely related to the physiological limits of the species, despite the uncertainty in the calculation of maximum drought stress. This is consistent with recent studies that have emphasised the importance of using climatic extremes rather than averages to explain ecological patterns, despite being well correlated (Stewart et al. 2021). Moreover, this agrees with Blackman et al. (2012) and Brodribb et al. (2014) who also showed this pattern when looking at correlation of Ψ_{50} with the 5th percentile of *map* or the driest quarter rainfall. Larter et al. (2017) and

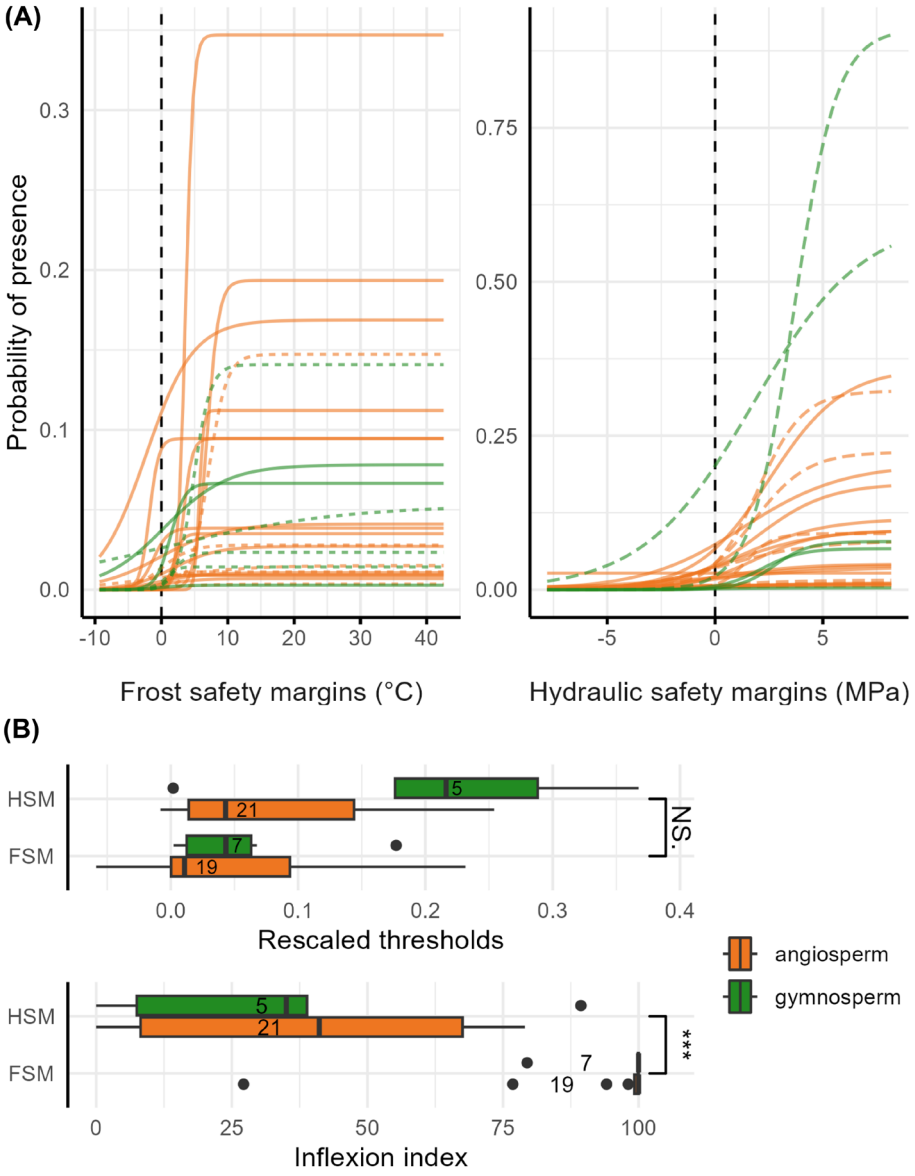

Figure 3. Predicted probability of presence as a function of FSM and HSM (A) and parameters of the function describing the shift in probability of presence – the rescaled threshold *t* and the inflection index *I*. (B). (A) Predictions are made from the mean model outputs, with the other safety margins fixed at their 95th percentiles. Colours highlight differences between angiosperms (orange) and gymnosperms (green). Dashed lines represent species with a model including only one safety margin. (B) Metrics of the model: thresholds *t* rescaled by the range of safety margin for the species, and the inflection index *I* calculated as the ratio between the slope *r* at the inflection point *t* and at 95th percentiles of the safety margin range. The number of species in each distribution is shown in the box plots. Differences between groups, i.e. HSM vs. FSM, were tested by t-test and, if significant, are indicated by *, ** or ***, corresponding to p-values less than 0.05, 0.01 and 0.001, respectively.

Skelton et al. (2021) reported that species with lower mean *map* were found to have greater resistance to embolism, whereas we found no significant relationship between Ψ_{50} and *map* percentiles. This could be because, unlike the above studies, we did not cover very arid environments. Other more complex variables (such as the precipitation in the driest months) could also have been tested to explain variations in Ψ_{50}, but here we focused on the most classical variables.

Fewer studies have investigated the environmental variability of species' frost tolerance traits. In particular, they have shown associations between cold stress resistance and niche minimum temperature (Zanne et al. 2018), potential elevation limits (Charrier et al. 2013), niche mean temperature and precipitation (Kreyling et al. 2015). In addition, Lancaster and Humphreys (2020) found a latitudinal cline for frost tolerance in different plant groups. A key advance of our study is to show that winter maximum frost hardiness is useful to standardise LT_{50} extracted from the literature for numerous species and capture species' distribution low-temperature limit.

Safety margins are relevant for explaining drop in species probability of presence

Differential sensitivity to frost and drought

Our analysis showed that species' probability of presence dropped before they reached their stress tolerance. In addition, crossing the frost tolerance threshold, LT_{50}, resulted in a steeper decrease in the probability of presence than for the drought threshold (Fig. 3).

Trees' responses to their frost safety margins indicate that they often operate close to their limits in terms of frost-induced cell damage during winter. This observation challenges previous studies that suggest trees have broad safety margins in winter (Körner et al. 2016). However, since our model is correlative, it does not demonstrate that winter frost-induced damage is the driving mechanism behind the cold range limits of species. Many other mechanisms could explain the cold range limits of species, such as embolisms caused by freeze–thaw cycles, late frosts that damage reproductive tissues or shorten growing season. (Morin et al. 2007, Charrier et al. 2017, Zanne et al. 2018). Winter LT_{50} could be indirectly correlated with these other frost-related limiting factors. Nevertheless, winter LT_{50} seems a relevant trait to capture interspecific variability in frost tolerance in a standardised way and is valuable for understanding species distributions.

The response to drought safety margins was less clear: thresholds were on average higher than zero, and non-linearity indices indicated a more progressive effect than for frost.

Moreover, the drop in the probability of presence was closer to the point where the species' drought tolerance is crossed for angiosperms than for gymnosperms. This pattern arises even though we used different Ψ_{crit} for angiosperms and gymnosperms to account for the anatomical and physiological differences between the two groups (Ψ_{88} for angiosperms and Ψ_{50} for gymnosperms). Previous studies have already shown that gymnosperms operate at greater hydraulic safety margins than angiosperms, highlighting the need for separate analyses of their drought resistance (Choat et al. 2012, Urli et al. 2013). This may explain the observed taxonomic differences.

The positive threshold and low non-linearity suggest that it is challenging to capture drought vulnerability in a single dimension. In fact, there are many different drought resistance strategies (Martin-StPaul et al. 2017, Choat et al. 2018). For example, in addition to embolism resistance, stomatal regulation is critical in controlling tree drought survival. Stomatal closure significantly reduces water loss, and the timing of this closure varies greatly between species, typically preceding extensive xylem embolism (Martin-StPaul et al. 2017). Residual water loss through leaf cuticle, bark and 'leaky' closed stomata also plays a key role in determining the timing of plant death during drought (Martin-StPaul et al. 2017). Leaf shedding could mitigate water loss during drought and allow angiosperms to reduce investment in xylem embolism resistance. Root function and its ability to disconnect from the soil may also play a critical role in some species. Furthermore, increased pathogen susceptibility during drought adds another layer of complexity to the situation (Trugman et al. 2021). In addition, unlike frost, drought is associated with water, a shared resource for which multiple species compete directly. The weaker effect of drought in our distribution models could also result from higher uncertainties in our metric of maximum drought stress compared to our metric of maximum frost stress. Indeed, soil water content is notoriously more difficult to estimate in climate reanalysis than temperature (Muñoz-Sabater et al. 2021, Velikou et al. 2022).

Yet, this differential response of probability of presence to frost and drought echoes studies comparing the role of frost versus heat tolerance. Araújo et al. (2013) and Lancaster and Humphreys (2020) highlighted greater variability in frost tolerance between lineages and a better link to species' latitudinal limits than for heat tolerance.

Distribution modelling at the interface between correlative and mechanistic models

We found that the distribution of most of our 38 species was related to their safety margins. Only the distribution of three species, *Juniperus communis*, *Populus alba* and *Quercus pubescens*, could not be explained by any of the safety margins.

Our model allowed us to introduce information from physiological traits into a correlative distribution model while maintaining a simplistic approach. As advocated in the review by Dormann et al. (2012), there is an urgent need to incorporate more physiology into correlative models. This is because mechanistic models perform better in novel climatic regimes and for species with limited occurrence data, whereas correlative models are more easily transferable across space and time (Dormann et al. 2012, Higgins et al. 2020). To bridge this gap, one strategy consist in calibrating physiological mechanistic models for numerous species (Chuine and Beaubien 2001, Martin-StPaul et al. 2017) to project species distributions forward. Mechanistic models can also be inversely calibrated from species occurrence data (Hartig et al. 2012) to more easily estimate the large number of parameters. Another strategy rooted in the correlative philosophy is to fit correlative SDMs with trait-dependant parameters (Pollock et al. 2012, Vesk et al. 2021). These traits-SDMs mostly rely on traits capturing leaf economics, establishment or competitive strategies, but do not enable interpretation of model parameters in terms of physiological processes. In animal ecology, the 'biophysical ecology' paradigm proposes to directly incorporate the link between functional traits and environments into SDMs, for example using as a predictor the difference between body temperature and maximum temperature (Kearney and Porter 2009).

Our safety margins are the equivalent of these predictors for tree species and our model uses a similar approach as 'biophysical ecology', to fit a correlational distribution model in a physiological stress space and account directly for the limits set by species physiological tolerance traits. This results in a simpler model than physiological mechanistic models, but still allows a good connection with physiological processes

and good transferability to species not included in the fit and for which only physiological traits information are available. Indeed, we found that when trying to predict the distribution of a species without presence/absence calibration data, our generic models based on safety margins gave AUC ranges similar to trait-SDMs (AUC median and interquartile of Vesk et al. 2021: 0.65 [0.57, 0.77]). It would be interesting to also test the predictive ability of our model in new continents or regions with a distinct species pool as in Vesk et al. (2021). We noted an average higher sensitivity of the model than specificity, highlighting the overpredicting trend of our models. This might be caused by constraints that safety margins could not catch, such as higher competition in species hot margins (Sexton et al. 2009).

The challenge of our safety margin approach is to find a good compromise in the simplification of physiological processes. Too much detail would lead to the complexity pitfalls of mechanistic models, while too much simplicity would produce indicators that are too coarse. For instance, it would be interesting to account for the duration and frequency of negative safety margins. The duration of drought stress is indeed important (Martin-StPaul et al. 2017), but remains difficult to include in safety margins.

Limitations of our study

Due to limited data availability, we did not consider intraspecific variability in physiological tolerance traits. Existing studies suggest modest intraspecific variability in LT_{50}, with populations at the cold extremes of the distribution exhibiting higher resistance (Morin et al. 2007). Studies of plasticity drivers of Ψ_{50} are very scarce and often focus on a few species (Anderegg 2015, González-Muñoz et al. 2018). When accounting for the high measurement errors, most studies concluded that this trait is strongly conserved (Lamy et al. 2014, Skelton et al. 2019) (but see Anderegg 2015). In addition, our analysis did not show a positive probability of occurrence for negative safety margins, which would be expected if plasticity allows species to be more tolerant in extreme environments.

Second, by choosing tolerance thresholds related to species survival, we assumed that species distribution is limited by this demographic process. However, numerous studies (Sexton et al. 2009, Hargreaves et al. 2014) have shown that distribution also depends on growth and reproduction. These complex mechanisms remain difficult to capture with physiological stress tolerance traits. Finally, our soil potentials map depends on the 9 × 9 km soil water content map, which is very crude to capture such a highly heterogeneous variable.

Conclusion

Our study is an important step towards building correlative models that are better constrained by physiological traits. The originality lies in modeling species distribution using physiological safety margins, derived from European climate reanalysis and frost and drought tolerance traits. It is a complementary approach to trait-SDMs, bridging the gap between correlative and mechanistic models. Our frost and drought safety margins pave the way for delimiting areas of tree species' ranges that are vulnerable to climate change.

Funding – This research is funded through the Pack Ambition Recherche 2020 VULCADYS of Region AURA (20 009534 01) and ANR DECLIC (grant ANR-20-CE32-0005-01). The PhD grant of AB was funded by the Pack Ambition Recherche 2020 VULCADYS. GK, TC, SD, ML, and GC were funded by ANR DECLIC (grant ANR-20-CE32-0005-01). GK was funded by RESONATE H2020 project (grant 101000574).

Author contributions

Anne Baranger: Conceptualization (lead), Data curation (lead), Formal analysis (lead), Methodology (lead), Writing - original draft (lead), Writing - review and editing (equal). **Thomas Cordonnier:** Funding acquisition (equal), Methodology (equal), Supervision (equal), Writing - review and editing (equal). **Guillaume Charrier**: Conceptualization (supporting), Data curation (supporting), Methodology (supporting), Writing - review and editing (supporting). **Sylvain Delzon**: Methodology (supporting), Resources (supporting), Writing - review and editing (supporting). **Maximilien Larter:** Methodology (supporting), Resources (equal), Writing - review and editing (supporting). **Nicolas K. Martin (stpaul):** Methodology (supporting), Writing - review and editing (supporting). **Georges Kunstler:** Conceptualization (equal), Funding acquisition (lead), Methodology (equal), Supervision (lead), Writing - review and editing (lead).

Transparent peer review

The peer review history for this article is available at https://www.webofscience.com/api/gateway/wos/peer-review/ecog.07528.

Data availability statement

Data are available from the Dryad Digital Repository: https://doi.org/10.5061/dryad.547d7wmh1 (Baranger et al. 2024).

Supporting information

The Supporting information associated with this article is available with the online version.

References

Allouche, O., Tsoar, A. and Kadmon, R. 2006. Assessing the accuracy of species distribution models: prevalence, kappa and the true skill statistic (TSS). – J. Appl. Ecol. 43: 1223–1232.

Anderegg, W. R. L. 2015. Spatial and temporal variation in plant hydraulic traits and their relevance for climate change impacts on vegetation. – New Phytol. 205: 1008–1014.

Anderegg, W. R. L., Flint, A., Huang, C. Y., Flint, L., Berry, J. A., Davis, F., Sperry, J. S. and Field, C. B. 2015. Tree mortality predicted from drought-induced vascular damage. – Nat. Geosci. 8: 367–371.
Araújo, M. B., Ferri-Yáñez, F., Bozinovic, F., Marquet, P. A., Valladares, F. and Chown, S. L. 2013. Heat freezes niche evolution. – Ecol. Lett. 16: 1206–1219.
Baranger, A., Cordonnier, T., Charrier, G., Delzon, S., Larter, M., Martin-StPaul, N. K. and Kunstler, G. 2024. Data from: Living on the edge – physiological tolerance to frost and drought explains range limits of 35 European tree species. – Dryad Digital Repository, https://doi.org/10.5061/dryad.547d7wmh1.
Benito Garzón, M., González Muñoz, N., Wigneron, J.-P. P., Moisy, C., Fernández-Manjarrés, J. and Delzon, S. 2018. The legacy of water deficit on populations having experienced negative hydraulic safety margin. – Global Ecol. Biogeogr. 27: 346–356.
Blackman, C. J., Brodribb, T. J. and Jordan, G. J. 2012. Leaf hydraulic vulnerability influences species' bioclimatic limits in a diverse group of woody angiosperms. – Oecologia 168: 1–10.
Brodribb, T. J., McAdam, S. A. M., Jordan, G. J. and Martins, S. C. V. 2014. Conifer species adapt to low-rainfall climates by following one of two divergent pathways. – Proc. Natl Acad. Sci. USA 111: 14489–14493.
Carpenter, B., Gelman, A., Hoffman, M. D., Lee, D., Goodrich, B., Betancourt, M., Brubaker, M. A., Guo, J., Li, P. and Riddell, A. 2017. Stan: a probabilistic programming language. – J. Stat. Softw. 76: 1.
Charra-Vaskou, K., Charrier, G., Wortemann, R., Beikircher, B., Cochard, H., Ameglio, T. and Mayr, S. 2012. Drought and frost resistance of trees: a comparison of four species at different sites and altitudes. – Ann. For. Sci. 69: 325–333.
Charrier, G., Cochard, H. and Améglio, T. 2013. Evaluation of the impact of frost resistances on potential altitudinal limit of trees. – Tree Physiol. 33: 891–902.
Charrier, G., Nolf, M., Leitinger, G., Charra-Vaskou, K., Losso, A., Tappeiner, U., Améglio, T. and Mayr, S. 2017. Monitoring of freezing dynamics in trees: a simple phase shift causes complexity. – Plant Physiol. 173: 2196–2207.
Choat, B., et al. 2012. Global convergence in the vulnerability of forests to drought. – Nature 491: 752–755.
Choat, B., Brodribb, T. J., Brodersen, C. R., Duursma, R. A., López, R. and Medlyn, B. E. 2018. Triggers of tree mortality under drought. – Nature 558: 531–539.
Chuine, I. and Beaubien, E. G. 2001. Phenology is a major determinant of tree species range. – Ecol. Lett. 4: 500–510.
Dormann, C. F., Schymanski, S. J., Cabral, J., Chuine, I., Graham, C., Hartig, F., Kearney, M., Morin, X., Römermann, C., Schröder, B. and Singer, A. 2012. Correlation and process in species distribution models: bridging a dichotomy. – J. Biogeogr. 39: 2119–2131.
Elith, J. and Leathwick, J. R. 2009. Species distribution models: ecological explanation and prediction across space and time. – Annu. Rev. Ecol. Evol. Syst. 40: 677–697.
Fielding, A. H. and Bell, J. F. 1997. A review of methods for the assessment of prediction errors in conservation presence/absence models. – Environ. Conserv. 24: 38–49.
Gelman, A., Carlin, J. B., Stern, H. S., Dunson, D. B., Vehtari, A. and Rubin, D. 2013 Bayesian data analysis, 3rd edn. – CRC Press, p. 677.
González-Muñoz, N., Sterck, F., Torres-Ruiz, J. M., Petit, G., Cochard, H., von Arx, G., Lintunen, A., Caldeira, M. C., Capdeville, G., Copini, P., Gebauer, R., Grönlund, L., Hölttä, T., Lobo-do-Vale, R., Peltoniemi, M., Stritih, A., Urban, J. and Delzon, S. 2018. Quantifying in situ phenotypic variability in the hydraulic properties of four tree species across their distribution range in Europe. – PLoS One 13: e0196075.
Hammond, W. et al. 2021. The global vulnerability of plant xylem. – In: AGUFM. 2021, pp. B31F–B07.
Hargreaves, A. L., Samis, K. E. and Eckert, C. G. 2014. Are species' range limits simply niche limits writ large? A review of transplant experiments beyond the range. – Am. Nat. 183: 157–173.
Hartig, F., Dyke, J., Hickler, T., Higgins, S. I., O'Hara, R. B., Scheiter, S. and Huth, A. 2012. Connecting dynamic vegetation models to data - an inverse perspective. – J. Biogeogr. 39: 2240–2252.
Hiederer, R. 2013. Mapping soil properties for Europe - spatial representation of soil database attributes. – EUR26082EN scientific and technical research series, 47: 1831-9424.
Higgins, S. I., Larcombe, M. J., Beeton, N. J., Conradi, T. and Nottebrock, H. 2020. Predictive ability of a process-based versus a correlative species distribution model. – Ecol. Evol. 10: 11043–11054.
Karger, D. N., Conrad, O., Böhner, J., Kawohl, T., Kreft, H., Soria-Auza, R. W., Zimmermann, N. E., Linder, H. P. and Kessler, M. 2017. Climatologies at high resolution for the earth's land surface areas. – Sci. Data 4: 170122.
Kearney, M. and Porter, W. 2009. Mechanistic niche modelling: combining physiological and spatial data to predict species' ranges. – Ecol. Lett. 12: 334–350.
Körner, C., Basler, D., Hoch, G., Kollas, C., Lenz, A., Randin, C. F., Vitasse, Y. and Zimmermann, N. E. 2016. Where, why and how? Explaining the low-temperature range limits of temperate tree species. – J. Ecol. 104: 1076–1088.
Kreyling, J., Schmid, S. and Aas, G. 2015. Cold tolerance of tree species is related to the climate of their native ranges. – J. Biogeogr. 42: 156–166.
Lamy, J.-B., Delzon, S., Bouche, P. S., Alia, R., Vendramin, G. G., Cochard, H. and Plomion, C. 2014. Limited genetic variability and phenotypic plasticity detected for cavitation resistance in a Mediterranean pine. – New Phytol. 201: 874–886.
Lancaster, L. T. and Humphreys, A. M. 2020. Global variation in the thermal tolerances of plants. – Proc. Natl Acad. Sci. USA 117: 13580–13587.
Larter, M., Pfautsch, S., Domec, J.-C., Trueba, S., Nagalingum, N. and Delzon, S. 2017. Aridity drove the evolution of extreme embolism resistance and the radiation of conifer genus *Callitris*. – New Phytol. 215: 97–112.
Lenz, A., Hoch, G., Vitasse, Y. and Körner, C. 2013. European deciduous trees exhibit similar safety margins against damage by spring freeze events along elevational gradients. – New Phytol. 200: 1166–1175.
Lindner, M., Fitzgerald, J. B., Zimmermann, N. E., Reyer, C., Delzon, S., van der Maaten, E., Schelhaas, M. J., Lasch, P., Eggers, J., van der Maaten-Theunissen, M., Suckow, F., Psomas, A., Poulter, B. and Hanewinkel, M. 2014. Climate change and European forests: what do we know, what are the uncertainties, and what are the implications for forest management? – J. Environ. Manage. 146: 69–83.
Lindström, A., Stattin, E., Gräns, D. and Wallin, E. 2014. Storability measures of Norway spruce and Scots pine seedlings and assessment of post-storage vitality by measuring shoot electrolyte leakage. – Scand. J. For. Res. 29: 717–724.
Mantova, M., Delzon, S., Rodriguez-dominguez, C. M., Ahmed, M. A., Trueba, S. and Torres-Ruiz, J. M. 2022. On the path

from xylem hydraulic failure to downstream cell death. – New Phytol.: 1–14.
Martínez-Vilalta, J., Santiago, L. S., Poyatos, R., Badiella, L., de Cáceres, M., Aranda, I., Delzon, S., Vilagrosa, A. and Mencuccini, M. 2021. Towards a statistically robust determination of minimum water potential and hydraulic risk in plants. – New Phytol. 232: 404–417.
Martin-StPaul, N., Delzon, S. and Cochard, H. 2017. Plant resistance to drought depends on timely stomatal closure. – Ecol. Lett. 20 : 1437–1447.
Mauri, A., Strona, G. and San-Miguel-Ayanz, J. 2017. EU-Forest, a high-resolution tree occurrence dataset for Europe. – Sci. Data 4: 160123.
Morin, X., Améglio, T., Ahas, R., Kurz-Besson, C., Lanta, V., Lebourgeois, F., Miglietta, F. and Chuine, I. 2007. Variation in cold hardiness and carbohydrate concentration from dormancy induction to bud burst among provenances of three European oak species. – Tree Physiol. 27: 817–825.
Muñoz-Sabater, J., Dutra, E., Agustí-Panareda, A., Albergel, C., Arduini, G., Balsamo, G., Boussetta, S., Choulga, M., Harrigan, S., Hersbach, H., Martens, B., Miralles, D. G., Piles, M., Rodríguez-Fernández, N. J., Zsoter, E., Buontempo, C. and Thépaut, J. N. 2021. ERA5-Land: a state-of-the-art global reanalysis dataset for land applications. – Earth Syst. Sci. Data 13: 4349–4383.
Nguyen, D. and Leung, B. 2022. How well do species distribution models predict occurrences in exotic ranges? – Global Ecol. Biogeogr. 31: 1051–1065.
Pollock, L. J., Morris, W. K., Vesk, P. A., Pollock, L. J. and Morris, W. K. 2012. The role of functional traits in species distributions revealed through a hierarchical model. – Ecography 35: 716–725.
Ruffault, J., Pimont, F., Cochard, H., Dupuy, J.-L. and Martin-StPaul, N. 2022. SurEauEcos v2.0: a trait-based plant hydraulics model for simulations of plant water status and drought-induced mortality at the ecosystem level. – Geosci. Model Dev. 15: 5593–5626.
Sakai, A. and Larcher, W. 1987. Mechanisms of frost survival. – In: Frost survival of plants: responses and adaptation to freezing stress. Springer, pp. 59–96.
Sanchez-Martinez, P., Martínez-Vilalta, J., Dexter, K. G., Segovia, R. A. and Mencuccini, M. 2020. Adaptation and coordinated evolution of plant hydraulic traits. – Ecol. Lett. 23: 1599–1610.
Sanchez-Martinez, P., Mencuccini, M., García-Valdés, R., Hammond, W. M., Serra-Diaz, J. M., Guo, W. Y., Segovia, R. A., Dexter, K. G., Svenning, J. C., Allen, C. and Martínez-Vilalta, J. 2023. Increased hydraulic risk in assemblages of woody plant species predicts spatial patterns of drought-induced mortality. – Nat. Ecol. Evol. 7: 1620–1632.
Schielzeth, H. 2010. Simple means to improve the interpretability of regression coefficients. – Methods Ecol. Evol. 1: 103–113.
Schwarz, G. 1978. Estimating the dimension of a model. – Ann. Statist. 6: 461–464.
Sexton, J. P., McIntyre, P. J., Angert, A. L. and Rice, K. J. 2009. Evolution and ecology of species range limits. – Annu. Rev. Ecol. Evol. Syst. 40: 415–436.
Skelton, R. P., Anderegg, L. D. L., Diaz, J., Kling, M. M., Papper, P., Lamarque, L. J., Delzon, S., Dawson, T. E. and Ackerly, D. D. 2021. Evolutionary relationships between drought-related traits and climate shape large hydraulic safety margins in western North American oaks. – Proc. Natl Acad. Sci. USA 118: e2008987118.
Skelton, R. P., Anderegg, L. D. L., Papper, P., Reich, E., Dawson, T. E., Kling, M., Thompson, S. E., Diaz, J. and Ackerly, D. D. 2019. No local adaptation in leaf or stem xylem vulnerability to embolism, but consistent vulnerability segmentation in a North American oak. – New Phytol. 223: 1296–1306.
Stewart, S. B., Elith, J., Fedrigo, M., Kasel, S., Roxburgh, S. H., Bennett, L. T., Chick, M., Fairman, T., Leonard, S., Kohout, M., Cripps, J. K., Durkin, L. and Nitschke, C. R. 2021. Climate extreme variables generated using monthly time-series data improve predicted distributions of plant species. – Ecography 44: 626–639.
Timmis, R., Flewelling, J. and Talbert, C. 1994. Frost injury prediction model for Douglas-fir seedlings in the Pacific Northwest. – Tree Physiol. 14: 855–869.
Tóth, B., Weynants, M., Pásztor, L. and Hengl, T. 2017. 3D soil hydraulic database of Europe at 250 m resolution. – Hydrol. Processes 31: 2662–2666.
Trugman, A. T., Anderegg, L. D. L., Anderegg, W. R. L., Das, A. J. and Stephenson, N. L. 2021. Why is tree drought mortality so hard to predict? – Trends Ecol. Evol. 36: 520–532.
Urli, M., Porté, A. J., Cochard, H., Guengant, Y., Burlett, R. and Delzon, S. 2013. Xylem embolism threshold for catastrophic hydraulic failure in angiosperm trees. – Tree Physiol. 33: 672–683.
Van Genuchten, M. T. 1980. A closed-form equation for predicting the hydraulic conductivity of unsaturated soils. – Soil Sci. Soc. Am. J. 44: 892–898.
Velikou, K., Lazoglou, G., Tolika, K. and Anagnostopoulou, C. 2022. Reliability of the ERA5 in replicating mean and extreme temperatures across Europe. – Water 14: 543.
Venturas, M. D., Todd, H. N., Trugman, A. T. and Anderegg, W. R. L. 2021. Understanding and predicting forest mortality in the western United States using long-term forest inventory data and modeled hydraulic damage. – New Phytol. 230: 1896–1910.
Vesk, P. A., Morris, W. K., Neal, W. C., Mokany, K. and Pollock, L. J. 2021. Transferability of trait-based species distribution models. – Ecography 44: 134–147.
Zanne, A. E., Pearse, W. D., Cornwell, W. K., McGlinn, D. J., Wright, I. J. and Uyeda, J. C. 2018. Functional biogeography of angiosperms: life at the extremes. – New Phytol. 218: 1697–1709.